EUKARYOTIC CELL, Sept. 2008, p. 1611–1615 Vol. 7, No. 9
1535-9778/08/$08.00+0 doi:10.1128/EC.00458-07

β1,2-Xylosyltransferase Cxt1p Is Solely Responsible for Xylose Incorporation into *Cryptococcus neoformans* Glycosphingolipids▽

Sherry A. Castle,[1] Elizabeth A. Owuor,[1] Stephanie H. Thompson,[1] Michelle R. Garnsey,[1] J. Stacey Klutts,[2,3]† Tamara L. Doering,[2] and Steven B. Levery[1]*

Department of Chemistry, University of New Hampshire, G229 Parsons Hall, Durham, New Hampshire 03824-3598,[1] and Departments of Molecular Microbiology[2] and Pathology and Immunology,[3] Washington University School of Medicine, St. Louis, Missouri 63110

Received 20 December 2007/Accepted 22 July 2008

The Manα1,3(Xylβ1,2)Manα structural motif is common to both capsular polysaccharides of *Cryptococcus neoformans* and to cryptococcal glycosphingolipids. Comparative analysis of glycosphingolipid structural profiles in wild-type and mutant strains showed that the Xylβ1,2-transferase (Cxt1p) that participates in capsular polysaccharide biosynthesis is also the sole transferase responsible for adding xylose to *C. neoformans* glycosphingolipids.

The pathogenic basidiomycete *Cryptococcus neoformans* causes serious disease in immunocompromised patients. A dominant feature of *C. neoformans* is its polysaccharide capsule, which is required for virulence. Xylose is a key component of both of the major polysaccharides comprising the capsule, glucuronoxylomannan (GXM) and galactoxylomannan (GalXM), and is essential for proper capsule formation and virulence (7, 16). Xylose is also a feature of *C. neoformans* glycosylinositol phosphorylceramides (GIPCs) (9), glycosphingolipids characteristic of fungi (4, 12). Fungal GIPCs differ fundamentally from mammalian glycosphingolipids in terms of structure, and their biosynthesis is essential for normal growth and life cycle (3, 5), suggesting they could be exploited for diagnostic (18) and therapeutic strategies (6, 17, 19). Interestingly, specific structural features are shared between the GIPCs and the capsular polysaccharides of *C. neoformans*. The GIPC core structure has the overall sequence Manα3(Xylβ2)Manα4Galβ6Manα2InsPCer (9). Like the structures of both GXM and GalXM, this structure includes a branching Xylβ1,2 residue linked to the reducing mannose of the Manα1,3Manα motif. In a more extensive parallel to GalXM, the xylosylated α-mannose of the GIPC core is 1,4-linked to β-galactose.

We have recently identified a cryptococcal Xylβ1,2-transferase (Cxt1p) that acts in synthesizing both capsule polysaccharides (11). Cells in which *CXT1* has been deleted (*cxt1*Δ::NAT [10]) show a 30% reduction in β1,2-Xyl addition to GXM and more than 90% reduction in β1,2-xylose addition to GalXM (10). In light of the structural homologies mentioned above, we tested the hypothesis that this enzyme also adds xylose to GIPCs. To do this, we compared GIPCs from a wild-type strain (JEC21) with those of the *cxt1*Δ mutant cells. As a control, we used a strain which bears the deletion of *UXS1*, the gene encoding UDP-GlcA decarboxylase (1, 16). This strain (*uxs1*Δ::*ADE2*) cannot synthesize the xylose donor UDP-xylose and is therefore globally deficient in the xylose modification of all glycoconjugates.

The *C. neoformans* JEC21, *uxs1*Δ (generously provided to the Doering laboratory by Guilhem Janbon) (16), and *cxt1*Δ strains (10) were grown at 30°C with rotation (200 rpm). All of these strains are closely related serotype D *MAT*α strains: the *cxt1*Δ strain was generated directly from JEC21, and the *uxs1*Δ strain was made from JEC155, which is derived from a related serotype D *MAT***a** strain (JEC20). For lipid preparations, cells were cultured in YPD medium (1% yeast extract, 2% Bacto peptone, 2% glucose) for 3 days, collected by centrifugation (6,000 rpm; 10 min; 4°C), washed once with cold water and twice with cold 20 mM sodium azide, and frozen. The frozen cell pellet (50 to 70 g [wet weight]) was then homogenized with 6 volumes of chloroform-methanol, 1:1 (vol/vol), and solvents were evaporated. Enrichment of glycosphingolipids, recov-

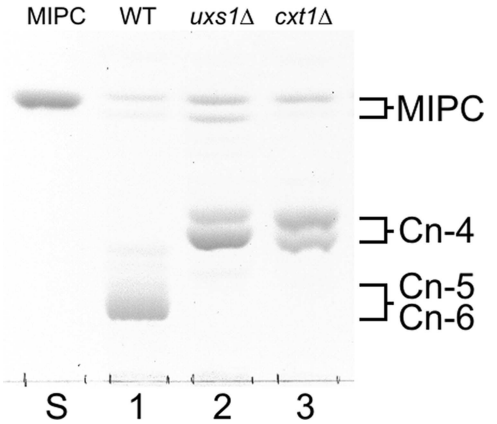

FIG. 1. HPTLC profiles of GIPCs (orcinol-stained acidic lipid fractions) from the *C. neoformans* strains indicated at the top of the lanes, along with authentic Manα2InsPCer (MIPC) standard from *Aspergillus fumigatus* (lane S). WT, wild-type strain JEC21. The origin is indicated by the line at the bottom of the image.

* Corresponding author. Present address: Department of Molecular and Cellular Medicine, University of Copenhagen, Blegdamsvej 3B, Copenhagen, 2200 N, Denmark. Phone: 45 3532 7779. Fax: 45 3536 7980. E-mail: levery@imbg.ku.dk.

† Present address: University of Iowa Carver College of Medicine, Iowa City, IA 52246.

▽ Published ahead of print on 1 August 2008.

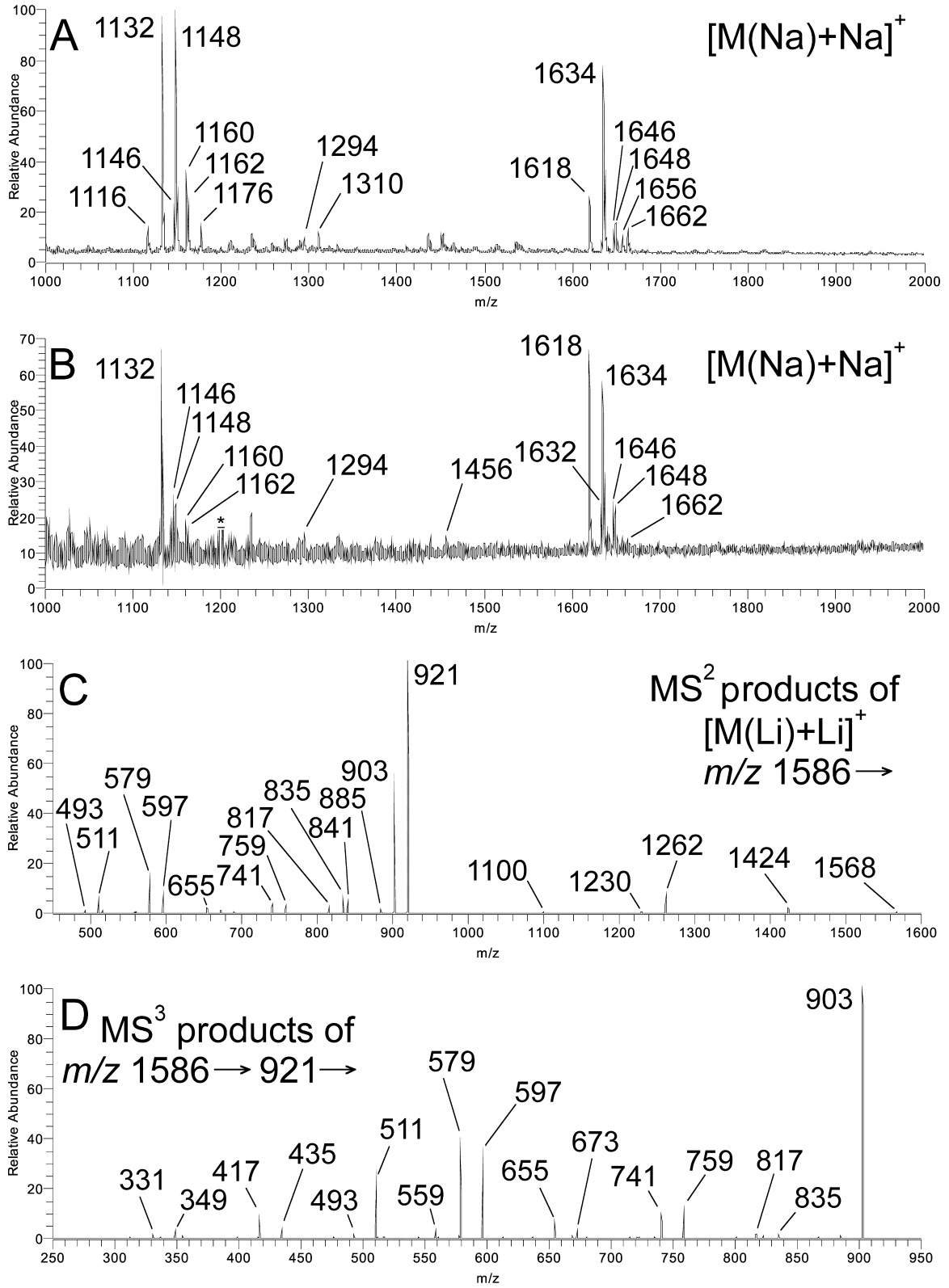

FIG. 2. Mass spectrometry of GIPC fractions. (A and B) $^{+}$ESI-MS^{1} profiles (as $[M(Na)+Na]^{+}$ salt adducts) of crude GIPC fractions from the *uxs1*Δ and *cxt1*Δ strains. (C) $^{+}$ESI-MS^{2} (*m/z* 1,586 →) spectrum of selected $[M(Li)+Li]^{+}$ salt adduct *m/z* 1,586 (Hex_4InsPCer, corresponding to the $[M(Na)+Na]^{+}$ salt adduct *m/z* 1,618 to 1632) in panel B. (D) $^{+}$ESI-MS^{3} (*m/z* 1,586 → 921 →) spectrum originating from the same molecular species.

TABLE 1. ESI-MS and ESI-MS^2 data for cryptococcal GIPCs[a]

Strain and GIPC	GIP t18:0/(fa)	MW (u) M(H)	*m/z*			
			$[M(Na)+Na]^+$	$[M(Li)+Li]^+$	$[Cer+Li]^+$	$[GIP(Li)+Li]^+$
WT (JEC21)						
Cn-1	HexInsP				435	
	(h24:0)	1,087	1,132	1,100		690
	($h_2$24:0)	1,103	1,148	1,116		706
Cn-5	Hex_4PenInsP				1,053	
	(h24:0)	1,705	1,750	1,718		690
	($h_2$24:0)	1,721	1,766	1,734		706
Cn-6	Hex_5PenInsP				1,215	
	(h24:0)	1,867	1,912	1,880		690
	($h_2$24:0)	1,883	1,928	1,896		706
*uxs1*Δ and *cxt1*Δ mutants						
Cn-1	HexInsP				435	
	(h24:0)	1,119	1,132	1,100		690
	($h_2$24:0)	1,135	1,148	1,116		706
Cn-4	Hex_4InsP				921	
	(h24:0)	1,573	1,618	1,586		690
	($h_2$24:0)	1,589	1,634	1,602		706

[a] MW, molecular weight; M(H), protonated uncharged molecular species; WT, wild type.

ery of acidic fractions containing GIPCs by ion-exchange chromatography, and purification of GIPCs by high-performance liquid chromatography were then performed as described previously (2, 18). Crude acidic fractions were analyzed by high-performance thin-layer chromatography (HPTLC) on silica gel no. 60 plates (E. Merck, Darmstadt, Germany) developed in chloroform-methanol-water (60:40:9 [vol/vol/vol], containing 0.002% [wt/vol] $CaCl_2$), with hexose-containing components detected by Bial's orcinol reagent.

Figure 1 shows the HPTLC profiles of GIPCs from the wild-type, the *uxs1*Δ, and the *cxt1*Δ cells. Each of the three strains exhibits a pair of bands that comigrates with a fungal Manα2InsPCer (MIPC) standard; the differences in the relative distribution of the bands between monohydroxy (upper) *N*-acyl forms and the dihydroxy (lower) *N*-acyl forms may reflect strain variation. (Consistent with this idea, the distribution of MIPC bands in the *cxt1*Δ strain is similar to that of the bands in JEC21, its immediate parent strain [Fig. 1, lanes 3 and 1, respectively]; distribution in the *uxs1*Δ strain [Fig. 1, lane 2] is somewhat altered.) Significantly, the wild-type cells also express major low-mobility components (Cn-5 and Cn-6) in a darkly stained band that is completely absent from both the *cxt1*Δ and the *uxs1*Δ cells. In contrast, the dominant product in the *cxt1*Δ strain is a pair of higher-mobility components (Cn-4) whose migration is consistent with that of compounds that are less polar than those of the major wild-type species. The pattern in the *uxs1*Δ strain, the control strain completely lacking UDP-xylose, is nearly identical. While this work was in progress, Gutierrez et al. (8) reported that the major GIPC species in the *uxs1*Δ cells is a truncated compound, Manα3Manα4Galβ6Manα2InsPCer. The production of the same species in the *cxt1*Δ cells (Fig. 1) demonstrates that Cxt1p is responsible for the transfer of all xylose to cryptococcal GIPCs.

We next performed structural studies to confirm the HPTLC comigration and identities of dominant products from the *uxs1*Δ and *cxt1*Δ strains. We first performed electrospray ion-

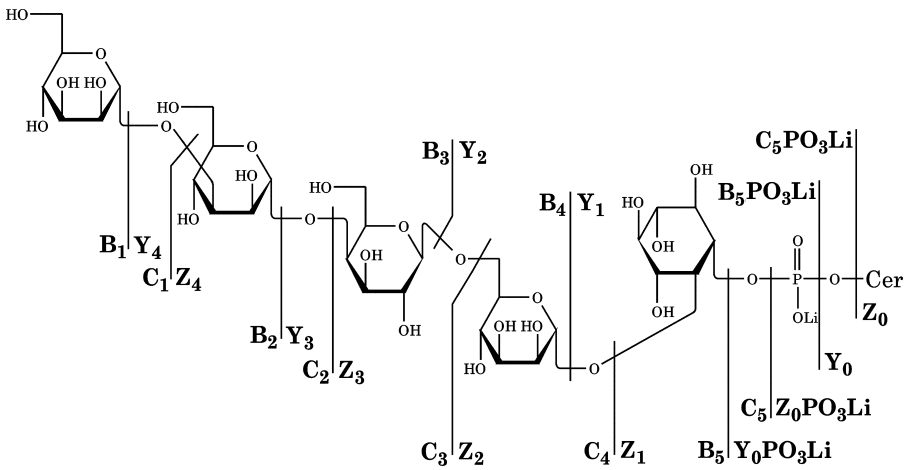

FIG. 3. Fragmentation of Manα3Manα4Galβ6Manα2InsPCer (Cn-4) in the modes $^+$ESI-MS^2 and $^+$ESI-MS^3.

TABLE 2. Product ions formed in low-energy ESI-MS^2 and ESI-MS^3 spectra[a]

m/z		Cn-4 assignment
h24:0	$h_2$24:0	
1,586	1,602	$[M(Li)+Li]^+$
1,568	1,586	$[M(Li)+Li-H_2O]^+$
1,424	1,440	$[M(Li)-Hex+Li]^+$
1,262	1,278	$[M(Li)-2Hex+Li]^+$
1,230	1,246	$[J(Li)+Li-H_2O]^+$
1,100	1,116	$[M(Li)-3Hex+Li]^+$
921		**$[C_5PO_3(Li)+Li]^+$**
903		**$[B_5PO_3(Li)+Li]^+$**
835		$[C_5+Li]^+$
817		$[B_5+Li]^+$
759		$[Y_4/C_5PO_3(Li)+Li]^+$
741		$[Y_4/B_5PO_3(Li)+Li]^+$
690	706	$[Y_0+Li]^+$
673		$[Y_4/C_5+Li]^+$ or $[C_4+Li]^+$
672		$[Z_0+Li]^+$
655		$[Y_4/B_5+Li]^+$ or $[B_4+Li]^+$
597		$[Y_3/C_5PO_3(Li)+Li]^+$
579		$[Y_3/B_5PO_3(Li)+Li]^+$
511		$[Y_3/C_5+Li]^+$ or $[Y_4/C_4+Li]^+$ or $[C_3+Li]^+$
493		$[Y_3/B_5+Li]^+$ or $[Z_3/C_5+Li]^+$ or $[Y_4/B_4+Li]^+$ or $[Z_4/C_4+Li]^+$ or $[B_3+Li]^+$
435		$[Y_2/C_5PO_3(Li)+Li]^+$
417		$[Y_2/B_5PO_3(Li)+Li]^+$
349		$[C_2+Li]^+$ or any equivalent two-residue segment
331		$[C_2+Li]^+$ or any equivalent two-residue segment

[a] Data show *m/z* of product ions formed in low-energy ESI-MS^2 and ESI-MS^3 spectra of lithium adducts of tetraglycosylinositol phosphorylceramide from *C. neoformans* GIPC (Cn-4). Base peaks are in boldface type, and fragment designations are shown as in references 2, 13, 15 and 18 and in Fig. 3.

ization mass spectrometry (ESI-MS and ESI-MS^n) to analyze crude and purified GIPC fractions in the positive ion mode ($^+$ESI), using a linear ion trap instrument (LTQ; Thermo Finnigan, San Jose, CA). Results were interpreted essentially as described in previous reports of purified GIPC components (2, 13–15, 18). Molecular profiles of *C. neoformans* GIPCs as $[M(Na)+Na]^+$ salt adducts were first acquired via $^+$ESI-MS. The compositions of the major molecular species in the JEC21 profile (not shown) were consistent with those of HexInsPCer (*m/z* 1,132, 1,148), Hex_4PenInsPCer (*m/z* 1,750, 1,766), and Hex_5PenInsPCer (*m/z* 1,912, 1,928). These results correspond to those of the previously characterized Manα2InsPCer (Cn-1), Manα3(Xylβ2)Manα4Galβ6Manα2InsPCer (Cn-5), and Manα6Manα3(Xylβ2)Manα4Galβ6Manα2InsPCer (Cn-6) GIPC sequences (9). The *m/z* difference of 16 between molecular adduct pair members is consistent with the differences between the degrees of hydroxylation of the ceramide fatty-*N*-acyl group (t18:0 4-hydroxy-sphinganine with h24:0 and $h_2$24:0 fatty acids, respectively). These results show that the low R_f band in the wild-type HPTLC profile (Fig. 1) corresponds to four components, Cn-5 and Cn-6, in an approximately 1:1 ratio, each bearing two types of ceramide. The profile of JEC21, thus, differs somewhat from those of the wild-type strains previously characterized (strain 444, which expressed Cn-5 almost exclusively, and strain KN99, which expressed Cn-6 almost exclusively [8, 9]).

The *uxs1*Δ and *cxt1*Δ mutant profiles are shown in Fig. 2A and B. Both profiles exhibit pairs of $[M(Na)+Na]^+$ salt adduct ions consistent with the HexInsPCer (*m/z* 1,132, 1,148) and Hex_4InsPCer (*m/z* 1,618, 1,634) compositions, corresponding to previously characterized GIPC sequences Manα2InsPCer (Cn-1) and Manα3Manα4Galβ6Manα2InsPCer (Cn-4) (8). We detected traces of components with intermediate numbers of Hex residues in the mutant GIPC profiles, but no trace of xylosylated GIPC products were detected in either mutant profile. These results are summarized in Table 1.

To confirm the lack of xylose in mutant GIPC molecular species, each molecular adduct in both profiles was selected for further fragmentation by the $^+$ESI-MS^n mode. To improve fragmentation, we treated the samples with lithium iodide, which converts GIPC molecular species to lithium salt adducts, $[M(Li)+Li]^+$ (2, 13, 15, 18); this also reduces the *m/z* of each molecular species by 32 compared with $[M(Na)+Na]^+$ (Table 1). A $^+$ESI-MS^2 spectrum acquired from the $[M(Li)+Li]^+$ peak at *m/z* 1,586 (corresponding to the $[M(Na)+Na]^+$ *m/z* 1,618) of the *cxt1*Δ mutant profile (Fig. 2C) showed the predominant glycosylinositol phosphate (GIP) fragment pair $[B_5PO_3(Li)+Li]^+/[C_5PO_3(Li)+Li]^+$ (*m/z* 921/903, respectively) corresponding to Hex_4InsP and other fragments from glycosidic cleavages (Fig. 3; Table 2). A ceramide ion ($[Y_0+Li]^+$) was observable at *m/z* 690 (the h24:0/t18:0 lipoforms, not marked). An $^+$ESI-MS^3 spectrum acquired from the $[C_5PO_3(Li)+Li]^+$ ion at *m/z* 921 (*m/z* 1,586 → 921 →) (Fig. 2D) showed that all of the glycosidic cleavages were consistent with those of a linear Hex_4InsP primary fragment (Fig. 3; Table 2). Essentially identical spectra were acquired from the $[M(Li)+Li]^+$ salt adduct at *m/z* 1,602 (corresponding to the $[M(Na)+Na]^+$ *m/z* 1,634; not shown), except that the ceramide ion was observed in the MS^2 spectrum at *m/z* 706 (the $h_2$24:0/t18:0 lipoforms). Essentially identical results were obtained from the corresponding pair of $[M(Li)+Li]^+$ salt adducts in the *uxs1*Δ strain profile (not shown).

Our data show that the lack of a single xylosyltransferase, Cxt1p, results in the complete absence of xylose from GIPCs of cryptococcal cells. This loss of xylose yields glycolipids that are indistinguishable from those formed in the *uxs1*Δ cells, where no xylose can be added to any glycans. The absence of residual xylose-containing GIPCs in the *cxt1*Δ mutant further indicates that no other enzyme performs the function of xylose addition during GIPC synthesis. In agreement with findings described by Gutierrez et al. (8), we observed that the lack of xylose modification of GIPC structures is accompanied by truncation of the terminal mannose residues distal to the branch.

Using in vitro assays, we have found that Cxt1p transfers xylose in β1,2 linkage to a Manα3Man disaccharide (11); our recent in vivo results further show that the *cxt1*Δ mutant is partially deficient in the transfer of Xylβ2 to both GXM and GalXM (10). Together, these data and the current studies demonstrate that Cxt1p is an unusual multiple-function xylosyltransferase that acts in three fundamental processes of *C. neoformans*: GXM synthesis, GalXM synthesis, and GIPC synthesis. The critical importance of the addition of xylose to cryptococcal biology and virulence (7, 16) suggests that this

fungus-specific protein warrants further investigation, in particular with respect to its role in cryptococcal pathogenesis.

This work was partially supported by an NIH grant (R21 RR20355) to S.B.L. Studies of cryptococcal glycan synthesis in the Doering laboratory are supported by NIH R01 awards GM71007 and GM66303 to T.L.D.

J.S.K. was supported by GM F32 072341 and a William Keck Foundation postdoctoral fellowship.

We thank Hong Liu for growth of *C. neoformans* and Vernon N. Reinhold for providing the MS facilities of the UNH Center for Structural Biology (NIH/NCRR grant no. P20 RR16459) for these studies.

REFERENCES

1. **Bar-Peled, M., C. L. Griffith, and T. L. Doering.** 2001. Functional cloning and characterization of a UDP-glucuronic acid decarboxylase: the pathogenic fungus *Cryptococcus neoformans* elucidates UDP-xylose synthesis. Proc. Natl. Acad. Sci. USA **98:**12003–12008.
2. **Bennion, B., C. Park, M. Fuller, R. Lindsey, M. Momany, R. Jennemann, and S. B. Levery.** 2003. Glycosphingolipids of the model fungus *Aspergillus nidulans*: characterization of GIPCs with oligo-α-mannose-type glycans. J. Lipid Res. **44:**2073–2088.
3. **Cheng, J., T.-S. Park, A. S. Fischl, and X. S. Ye.** 2001. Cell cycle progression and cell polarity require sphingolipid biosynthesis in *Aspergillus nidulans*. Mol. Cell. Biol. **21:**6198–6209.
4. **Dickson, R. C., and R. L. Lester.** 1999. Yeast sphingolipids. Biochim. Biophys. Acta **1426:**347–357.
5. **Dickson, R. C., and R. L. Lester.** 2002. Sphingolipid functions in *Saccharomyces cerevisiae*. Biochim. Biophys. Acta **1583:**13–25.
6. **Georgopapadakou, N. H.** 2000. Antifungals targeted to sphingolipid synthesis: focus on inositol phosphorylceramide synthase. Expert Opin. Investig. Drugs **9:**1787–1796.
7. **Griffith, C. L., J. S. Klutts, L. Zhang, S. B. Levery, and T. L. Doering.** 2004. UDP-glucose dehydrogenase plays multiple roles in the biology of the pathogenic fungus *Cryptococcus neoformans*. J. Biol. Chem. **279:**51669–51676.
8. **Gutierrez, A. L., L. Farage, M. N. Melo, R. S. Mohana-Borges, Y. Guerardel, B. Coddeville, J. M. Wieruszeski, L. Mendonca-Previato, and J. O. Previato.** 2007. Characterization of glycoinositolphosphoryl ceramide structure mutant strains of *Cryptococcus neoformans*. Glycobiology **17:**1–11C.
9. **Heise, N., A. L. S. Gutierrez, K. A. Mattos, C. Jones, R. Wait, J. O. Previato, and L. Mendonca-Previato.** 2002. Molecular analysis of a novel family of complex glycoinositolphosphoryl ceramides from *Cryptococcus neoformans*: structural differences between encapsulated and acapsular yeast forms. Glycobiology **12:**409–420.
10. **Klutts, J. S., and T. L. Doering.** 2008. Cryptococcal xylosyltransferase 1 (Cxt1p) from *Cryptococcus neoformans* plays a direct role in the synthesis of capsule polysaccharides. J. Biol. Chem. **283:**14327–14334.
11. **Klutts, J. S., S. B. Levery, and T. L. Doering.** 2007. A β-1,2-xylosyltransferase from *Cryptococcus neoformans* defines a new family of glycosyltransferases. J. Biol. Chem. **282:**17890–17899.
12. **Lester, R. L., and R. C. Dickson.** 1993. Sphingolipids with inositolphosphate-containing head groups. Adv. Lipid Res. **26:**253–274.
13. **Levery, S. B.** 2005. Glycosphingolipid structural analysis and glycosphingolipidomics. Methods Enzymol. **405:**300–369.
14. **Levery, S. B., M. S. Toledo, A. H. Straus, and H. K. Takahashi.** 1998. Structure elucidation of sphingolipids from the mycopathogen *Paracoccidioides braziliensis*: an immunodominant β-galactofuranose residue is carried by a novel glycosylinositol phosphorylceramide antigen. Biochemistry **37:**8764–8775.
15. **Levery, S. B., M. S. Toledo, A. H. Straus, and H. K. Takahashi.** 2001. Comparative analysis of glycosylinositol phosphorylceramides from fungi by electrospray tandem mass spectrometry with low-energy collision-induced dissociation of Li^+ adduct ions. Rapid Commun. Mass Spectrom. **15:**2240–2258.
16. **Moyrand, F., B. Klaproth, U. Himmelreich, F. Dromer, and G. Janbon.** 2002. Isolation and characterization of capsule structure mutant strains of *Cryptococcus neoformans*. Mol. Microbiol. **45:**837–849.
17. **Nagiec, M. M., E. E. Nagiec, J. A. Baltisberger, G. B. Wells, R. L. Lester, and R. C. Dickson.** 1997. Sphingolipid synthesis as a target for antifungal drugs. Complementation of the inositol phosphorylceramide synthase defect in a mutant strain of *Saccharomyces cerevisiae* by the *AUR1* gene. J. Biol. Chem. **272:**9809–9817.
18. **Toledo, M. S., S. B. Levery, B. Bennion, L. L. Guimaraes, S. A. Castle, R. Lindsey, M. Momany, C. Park, A. H. Straus, and H. K. Takahashi.** 2007. Analysis of glycosylinositol phosphorylceramides expressed by the opportunistic mycopathogen *Aspergillus fumigatus*. J. Lipid Res. **48:**1801–1824.
19. **Zhong, W., M. W. Jeffries, and N. H. Georgopapadakou.** 2000. Inhibition of inositol phosphorylceramide synthase by aureobasidin A in *Candida* and *Aspergillus* species. Antimicrob. Agents Chemother. **44:**651–653.